STRENGTH ANALYSIS OF FEMORAL IMPLANT OF BONE ANCHORED PROSTHESIS

Kithalawalana Jayathilaka[1], Oskars Gainutdinovs[2], Svetlana Sokolova[1], Peteris Studers[3]
[1]Riga Technical University, Latvia; [2]SIA "Tehniskā Ortopēdija", Latvia;
[3]Riga Stradins University, Latvia
kithalawalana@gmail.com, gainutdinovs@inbox.lv, svetlana.sokolova@rtu.lv

Abstract. Osseointegration is a ground-breaking medical technique that has transformed the field of prosthetics, particularly in the context of limb replacement. It involves the direct integration of an artificial implant, typically a metal rod, into the patient's residual bone, enabling a secure and stable connection for prosthetic limbs. This innovation has brought significant improvements in the lives of amputees, enhancing their mobility, comfort, and overall quality of life. One of the most significant advantages of osseointegration is the restoration of a more natural and intuitive limb movement. Traditional prosthetic limbs rely on sockets that are strapped to the residual limb, often leading to discomfort and a lack of proprioception. In contrast, osseo integrated prosthetics allow users to regain a closer approximation of their natural limb function, enhancing their ability to walk, run, and perform various daily tasks with ease. This paper is dedicated to the examination of the strength characteristics through stress simulations and fatigue calculations of a bone implant. The objective is to assess the implant capacity to withstand the load imposed by an amputee weighing 100 kg, ensuring structural integrity and preventing failure. The 3D model utilised in SolidWorks simulations was developed using data acquired from the analysis of 31 femur bones. These bones were examined through X-ray imaging in both Anteroposterior (AP) and Lateral (LAT) views, yielding a total of 62 analysed X-rays. Each X-ray image underwent meticulous analysis and measurements using the AutoCAD to determine the angles and distances between the bone canal axis and the mechanical axis. Subsequently, these individual values were amalgamated to derive a singular resultant angle and distance, which served as the basis for all subsequent simulations and calculations. The results could be used as a foundation for any research looking to examine and further study the strengths of a femoral implant.

Keywords: femoral implant, bone-anchored prosthesis, strength analysis, static simulations.

Introduction

Osseointegration and bone implants played vital roles in medical practice for decades, stemming from dental implant procedures [1; 2] and capturing the attention of engineers and surgeons. Over time, osseointegrated implantation advanced significantly [3], becoming a key treatment method for limb amputations. This biomechanical progress not only boosted durability but also enhanced the mobility and overall quality of life for amputees.

Despite advancements [4; 5], osseointegrated implantation was not widely recognized outside Europe due to the lack of standardized regulatory frameworks. Clinics had varying requirements and assessments for this procedure. A study aimed to establish a foundational framework for standardizing femoral bone implants, allowing manufacturers and clinics to use mechanical research findings as guidelines for a uniform model.

Utilising the PubMed search engine, it was found that there is a lack of research specifically addressing the strength analysis of femoral lower limb implants with similar geometric characteristics. Although numerous studies have explored hip and other implant analyses, a comprehensive investigation into the strength of femoral lower limb implants, encompassing the measurement of actual bone structures and diameter calculations, has not been previously undertaken.

This mechanical investigation focused mainly on strength calculations, stress simulations, and fatigue assessments of a bone implant with the minimum diameter to support a 100 kg [6; 7] amputee without structural failure. Analytical and simulated results were carefully analysed for thorough understanding. Standardising the minimum diameter of implants, especially those made from the expensive material Ti-6Al-4V, offered potential economic benefits for amputees by potentially reducing manufacturing costs for implant producers.

This study collaborated with Dr. Oskars Gainutdinovs, an Orthopaedic Surgeon from Orto Klīnika in Riga, Latvia. All medical specimens were obtained with proper authorization. The main aim was to establish a standard minimum diameter for femoral implants based on collected specimens. The methodology involved determining the minimum diameter where the bending moment on the implant was highest. It is worth noting that the femur bone had a non-perpendicular structural orientation, causing an angular deviation from the mechanical axis where body weight was primarily distributed.

Research specimens

In this study, 31 femur bones were analysed to measure the angles and distances between the bone canal axis (shown in green in Fig. 1) and the mechanical axis (shown in red in Fig. 1). This data was used to calculate an average value, which informed the calculation of the bending moment. A total of 62 X-rays of the femur bones were evaluated using the AutoCAD software program.

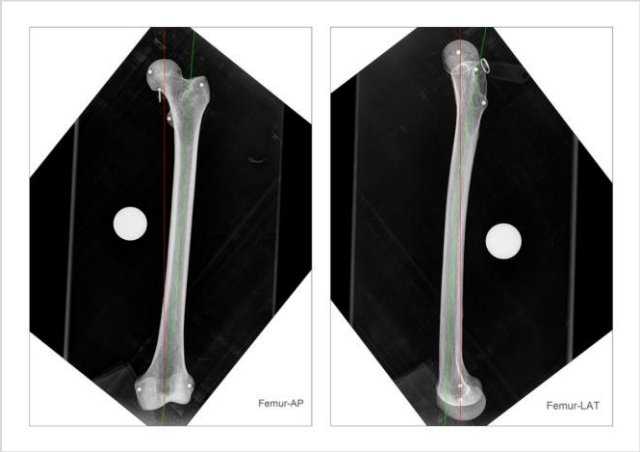

Fig. 1. **X-ray images of a femur bone in Anterior-Posterior (AP) and Lateral (LAT) views**

Methodology

Each X-ray image was imported into the computer-aided design software AutoCAD. The mechanical axis of the bone was divided into 20 equal cross-sectional levels. For each level, the angle between the bone canal axis and mechanical axis was measured, along with the perpendicular distance from the centre point of each level bone canal axis to the mechanical axis.

In the AP view, if the segment of the bone canal axis formed an acute angle with the mechanical axis on the medial side, the angle was deemed positive. Conversely, if the segment of the bone canal axis formed an acute angle on the lateral side, the angle was considered negative. Likewise, when the distance was situated on the lateral side of the mechanical axis, it was regarded as positive; conversely, when located on the medial side, it was deemed negative. However, it is noteworthy that in the AP view distances were predominantly positive. The same protocol was applied for measurements in the LAT view. Unlike the AP view, the LAT view exhibited both negative and positive distances.

As depicted by Fig. 2, it was how each specimen x-ray image looked in each view after the full measurement process was completed. All measurements from the 20 cross-sectional levels of each of the 31 bone specimens, obtained from both the Anteroposterior (AP) and Lateral (LAT) views, were aggregated to compute an average value for each of the cross-sectional levels. Subsequently, uncertainties with 95% confidence intervals were determined for these average values at each cross-sectional level.

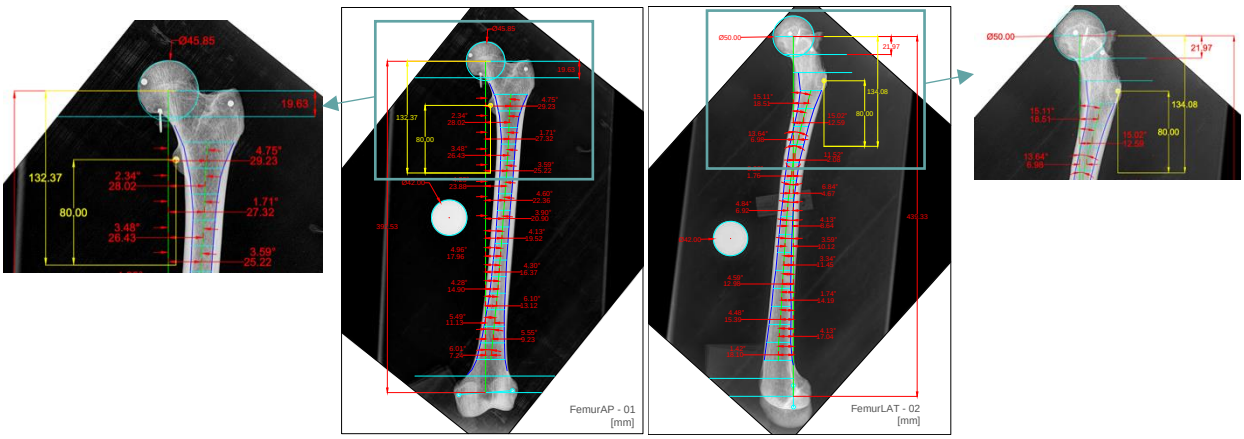

Fig. 2. **Completely measured LAT view and AP view of the x-ray no-02**

Average values were used to compute a resultant angle and distance by combining data from both views. The Pythagorean theorem was applied for distance calculations. Additionally, an average height percentage (referred to as "h" in Fig. 3) of the implant position was calculated and included in the strength calculations.

In current practice, femoral implants are restricted to amputees weighing a maximum of 100 kg according to the Integrum "OPRA Implant System" and The USA Food and Drug Administration (FDA) [6; 7], with a residual limb length of at least 8 cm from the "trochanter-minor". Finally, two graphs were generated (Fig. 4): one depicting "α vs% height of the mechanical axis" and the other "d vs% height of the mechanical axis". These graphs were utilised to determine the corresponding "α" and "d" values for the average "h" percentage previously calculated.

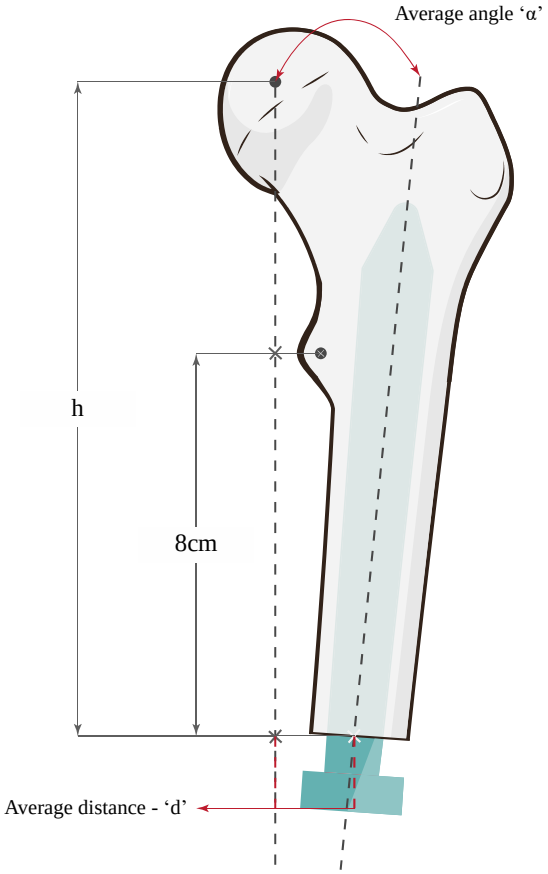

Fig. 3. **Femoral implant accompanied by the respective angle and distance measurements between the mechanical axis and the bone canal axis**

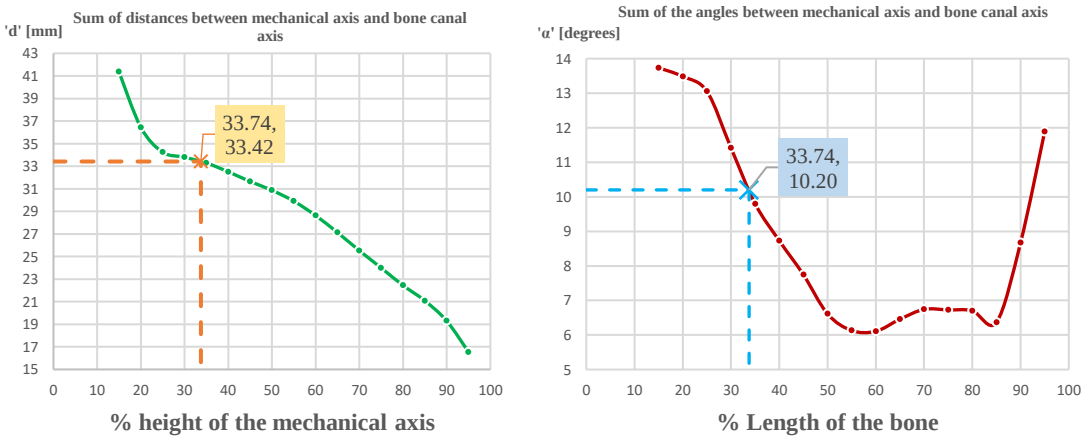

Fig. 4. **Left graph "d" and right graph "α" against% height of the mechanical axis**

Based on the data presented in Fig. 4 above, strength calculations for compression and bending were conducted by strength of material methods, giving the minimum diameter as 12.97 mm (Fig. 5).

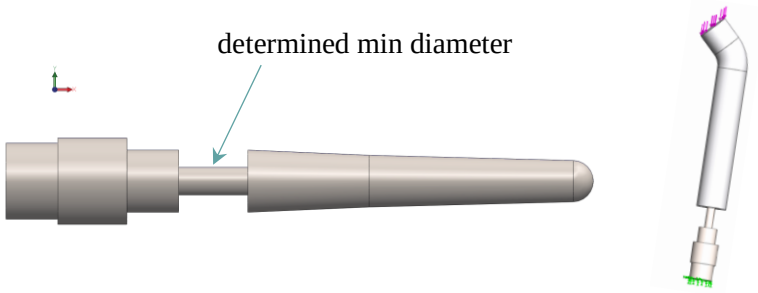

Fig. 5. **Femoral bone implant model and "bone-implant" model boundary conditions of SolidWorks simulation**

Strength simulation

Biomechanics integrates core mechanical engineering principles, including statics, dynamics, strength of materials, and finite element modelling, with the finite element method (FEM) being prominent [8]. SolidWorks software, based on FEM, simulated the strength of the "bone-implant" system. The finite element mesh consisted of tetrahedral elements, ensuring consistency and coinciding mesh nodes at contact points. Boundary conditions specified the implant end as fixed, with a load applied to the "bone" (see Fig. 5). A load of 2500N was determined based on previously published data concerning the range of movements and associated bending moments experienced by amputees in their daily activities [9-11]. The implant material, Ti-6Al-4V, had its properties pre-defined in SolidWorks. The bone model included three components, carefully chosen to ensure reliable results: a hollow cylindrical part for implant insertion and two additional elements closely mimicking femur bone structural characteristics, with corresponding mechanical properties.

Table 1

Femur bone mechanical properties

Elastic Modulus	Poisson's Ratio	Shear Modulus	Mass Density	Tensile Strength	Compressive Strength	Yield Strength
27800 MPa	0.33	10500 MPa	2100 kg·m^{-3}	136 MPa	136 MPa	129 MPa

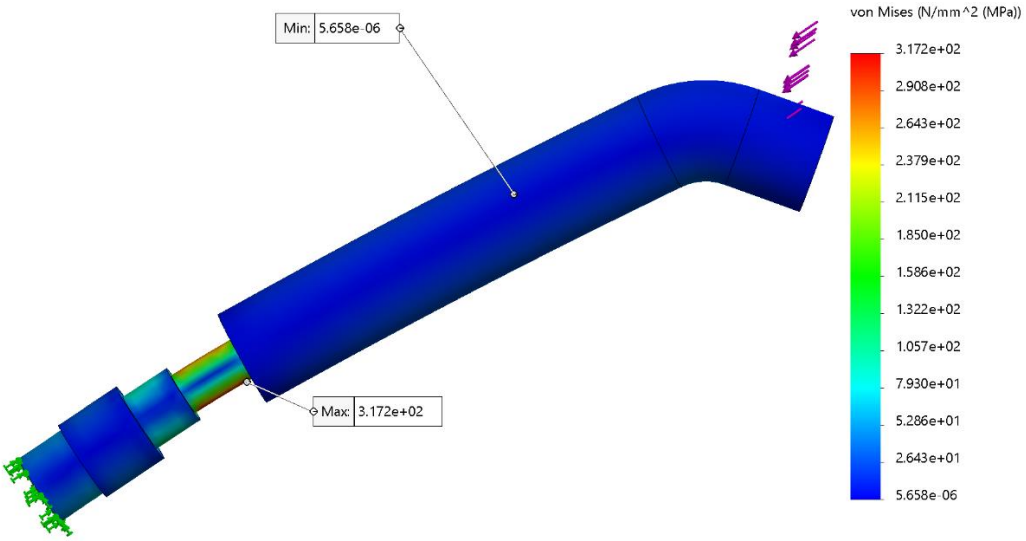

Fig. 6. **Femoral implant inserted femur bone static simulation in SolidWorks**

The maximum stress induced by a 2500 N force reached only 317.2 MPa (see Fig. 6). This was notably below the maximum yield strength of the implant material, Ti-6Al-4V, which stood at 827.37 MPa. Hence, the actual stress remained below the material yield strength, affirming that the

calculated minimum diameter of 12.97 mm could safely support the individual's weight, even under full concentration on one leg.

The safety factor for static loading was simulated at 2.6, indicating the structure's safety under static loading conditions. Dynamic loading testing was conducted on the implant. Fatigue simulations using SolidWorks [12; 13] were followed by analytical verification using the Goodman relation. The fatigue simulation (Fig. 7) revealed a minimum fatigue load factor of 34.27, confirming the model resilience against fatigue failure under a 2500N load.

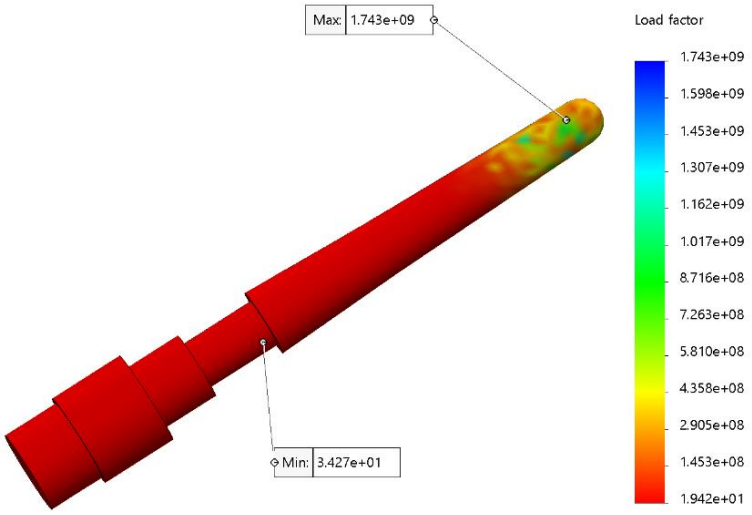

Fig. 7. **Femoral implant fatigue simulation load factor plot in SolidWorks**

Simulation of prestress

Contact interaction was specified between the "bone" and implant to simulate prestress. The level of prestress was modelled using temperature analogy (examples of such an approach in [14-16]). The "implant" had a coefficient of thermal expansion equal to $2.3 \cdot 10^{-5}$ K^{-1}. The level of prestress depends on the difference between the set and reference temperatures.

In the frequency range 0 to 500 Hz with zero prestress, one natural frequency was found to be equal to 145.3 Hz. With increasing prestress, the value of the natural frequency decreased (Fig. 8). To compare the mechanical and thermodynamic values, the second horizontal axis shows the value of the maximum radial displacement of the bone surface in the contact zone with the implant in accordance with the applied temperature.

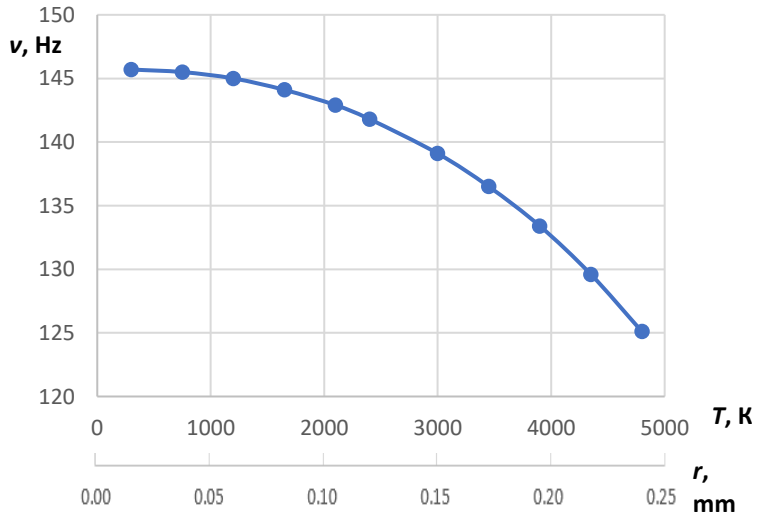

Fig. 8. **Relationship between the value of the first natural frequency and the prestress level (temperature)**

The decrease in the natural frequency with an increase in the prestress level was associated with the areas of compressive stresses in the “bone”, resulting in a decrease in its stiffness.

Results and discussion

This study involved an experimental assessment of the angles and distances between the mechanical axis of the femur bone and the bone canal axis. The graphical representation of these findings served to bolster their reliability. Strength calculations yielded a theoretical minimum diameter for the Ti-6Al-4V implant, which was subsequently validated through finite element analysis (FEA) conducted in SolidWorks. Stress simulations revealed that maximum stresses remained below ultimate stress levels, ensuring the structural integrity of the implant. Static and dynamic loading safety factors, determined via SolidWorks and the Goodman relation, further corroborated the safety of the implant. These findings validate the accuracy of the research methodology employed.

Suggestions

The findings from measurements and analysis of 31 femur bones laid the groundwork for future studies on femoral implant strength. It was also advised to use 3-D scans of femur specimens for improved accuracy in Finite Element Analysis (FEA) simulations.

Limitations

A key limitation faced during the research was the lack of data on the bone specimens, particularly regarding the age, gender, and lifestyles of the femur bone owners. Access to such information could have led to more accurate outcomes and potentially allowed for correlations between the bone mechanical properties and demographic factors to be established.

Recommendations

Future studies are recommended to concentrate on assessing and improving implant designs to withstand increased impact forces and endure higher stresses, reducing the risk of bone damage from accidents experienced by amputees in their daily lives.

Conclusions

The aim of this study was to establish the minimum diameter needed for a femoral implant in individuals weighing 100 kg with a residual limb length exceeding 8 cm. Using 32 femur bone specimens and 62 x-rays, the length and angle formed between the implant and the mechanical axis were determined at 33.42 mm and 10.20 degrees, respectively. Strength calculations factored in both compression and bending moments, deriving a minimum diameter of 12.97 mm for the implant material. This serves as a benchmark for future research on femoral implant strength.

Finite Element Analysis (FEA) simulations identified the highest stress point at the implant site in the femoral limb. However, the 12.97 mm diameter implant demonstrated superior ultimate strength, preventing failure despite the stress induced by loading conditions. This highlights the need to incorporate stress and loading factors into future implant designs to improve durability and safety.

Furthermore, the implant resistance to static and dynamic loading was thoroughly evaluated using analytical methods and computer simulations with SolidWorks. Both approaches confirmed the safety of the 12.97 mm diameter implant against failure under various loading conditions. Importantly, this study focused solely on establishing the minimum implant diameter to support the wearer’s weight, excluding external impacts or accidents. Future studies could investigate these aspects by examining larger implant diameters.

Acknowledgements

We express sincere gratitude to Dr. Vladislavs Jevstigņejevs from the Riga Technical University for his invaluable scientific guidance during this research. Dr. Jevstigņejevs’ expertise enriched the analysis and interpretation of femoral implant strength aspects. His mentorship significantly shaped this paper.

Author contributions

Conceptualization, O G; methodology, K J and S S; software, K J; validation, P S and O G; formal analysis, K J and S S; investigation, K J and S S; data curation, K J and S S; writing – original draft preparation, K J; writing – review and editing, K J and S S; visualization, P S; project administration, O G and K J; funding acquisition, O G. All authors have read and agreed to the published version of the manuscript.

References

[1] Branemark P., Zarb G., Albrektsson T. Tissue-Integrated Prostheses: Osseointegration in Clinical Dentistry. 1st ed. Chicago: Quintessence Publiishing; 1985.
[2] Brånemark R., Brånemark P.I., Rydevik B., Myers R.R. Osseointegration in skeletal reconstruction and rehabilitation: a review. J Rehabil Res Dev. 38, 2001, pp. 175-181.
[3] Integrum, "US Food and Drug Administration," [online] [11.02.2024]. Available at: https://www.accessdata.fda.gov/cdrh_docs/pdf8/H080004S002D.pdf.
[4] Reif T.J., Khabyeh-Hasbani N., Jaime K.M., Sheridan G.A., Otterburn D.M., Rozbruch S.R. Early experience with femoral and tibial bone-anchored osseointegration prostheses. JBJS Open Access. 2021;6:e21.00072. DOI: 10.2106/JBJS.OA.21.00072.
[5] Muderis M.A., Lu W., Tetsworth K., Bosley B., Li J.J. Single-stage osseointegrated reconstruction and rehabilitation of lower limb amputees: the Osseointegration Group of Australia Accelerated Protocol-2 (OGAAP-2) for a prospective cohort study. BMJ Open. 2017;7:e013508. DOI: 10.1136/bmjopen-2016-013508.
[6] Integrum OPRA Implant System, "US Food and Drug Administration," [online] [11.02.2024]. Available at: https://www.accessdata.fda.gov/cdrh_docs/pdf8/H080004S002C.pdf.
[7] Sreedharan S., Gray S., Bruscino-Raiola F. Osseointegrated prostheses for lower limb amputees: a review of complications. Australas J Plast Surg. 4(1), 2021, pp. 56-63. DOI: 10.34239/ajops.v4n1.199
[8] Mihçin Ş., Ciklacandir S. Towards integration of the finite element modeling technique into biomedical engineering education. Biomedical Engineering: Applications, Basis and Communications. 2022 Apr 3;34(02):2150054.
[9] Frossard L., Leech B., Pitkin M. Loading Applied on Osseointegrated Implant by Transtibial Bone-Anchored Prostheses During Daily Activities: Preliminary Characterization of Prosthetic Feet. Journal of Prosthetics and Orthotics 32(4), 2020, pp. 258-271. DOI: 10.1097/JPO.0000000000000280
[10] Lee W.C., Frossard L.A., Hagberg K., Haggstrom E., Brånemark R., Evans J.H., Pearcy M.J. Kinetics of transfemoral amputees with osseointegrated fixation performing common activities of daily living. Clin Biomech (Bristol, Avon). 2007 Jul; 22(6), pp. 665-673. DOI: 10.1016/j.clinbiomech.2007.02.005. Epub 2007 Apr 2. PMID: 17400346.
[11] Mihcin S., Sahin A.M., Yilmaz M. et al. Database covering the prayer movements which were not available previously. Sci Data 10, 276, 2023. DOI: 10.1038/s41597-023-02196-x
[12] Janeček M., Novy F., P. Harcuba F., Stráský J., Trško L., Mhaede M. Wagner L. "The Very High Cycle Fatigue Behaviour of Ti-6Al-4V Alloy," Acta Physica Polonica A, vol. 128, 2015, pp. 497-503.
[13] Hosseini S. "Fatigue of Ti-6Al-4V," 6 September 2012. DOI: 10.5772/45753.
[14] Urevc J., Brumen M., Flis V., Štok B. Applying Thermomechanical Analogy to Predict the Arterial Residual Stress State. Journal of Mechanical Engineering 61, 2015, pp. 5-23.
[15] Timoshenko S. History of Strength of Materials, Dover Publications, 1983.
[16] Abdelatifn A.O., Owen J.S., Hussein M.F.M. Modelling the prestress transfer in pre-tensioned concrete elements. Finite Elements in Analysis and Design 94, 2015, pp. 47-63.